

# Table Salt as a Template to Prepare Reusable Porous PVDF–MWCNT Foam for Separation of Immiscible Oils/Organic Solvents and Corrosive Aqueous Solutions

Faze Chen, Yao Lu, Xin Liu,\* Jinlong Song, Guanjie He, Manish K. Tiwari, Claire J. Carmalt, and Ivan P. Parkin\*

Many advanced materials are designed for separation of immiscible oils/organic solvents and aqueous solutions, including poly(vinylidene fluoride) (PVDF)-based materials with superwettability. However, due to the limited solubility of PVDF, techniques (e.g., phase inversion and electrospinning) often involve the use of toxic organic solvents. Here a facile organic solvent-free method is described to prepare a porous PVDF–MWCNT (multiwalled carbon nanotube) foam using table salt as a sacrificial template. The porous PVDF–MWCNT foam is characterized as superhydrophobic–superoleophilic with good elasticity due to its 3D porosity and low surface energy. The foam exhibits high adsorption capacity to a variety of oils/organic solvents and can be easily reused by squeezing, heating, or releasing in other solvents. Moreover, the foam is highly resistant toward UV exposure, corrosive aqueous solutions such as acidic, alkaline, salty solutions, and turbulent environments, and shows effective oils/organic solvents removal in these complex environments. The continuous separation of immiscible oils/organic solvents and corrosive aqueous solutions with vacuum assistance is also presented. The organic solvent-free and reusable PVDF–MWCNT foam is a promising candidate for large-scale industrial separation of oils/organic solvents and water in corrosive and turbulent conditions.

superoleophilicity have been introduced to separate immiscible oils/organic solvents and water-based solutions because of their excellent selective repellence (or affinity) toward water or oils/organic solvents.<sup>[2]</sup> According to the separation mode, these materials can be broadly classified into two categories. One is to build a separating filtration that from an oils/organic solvent and water mixture only allows either oil/organic solvent or water to go through but stops the other liquid, such as superhydrophobic–superoleophilic or superhydrophilic–superoleophobic meshes and membranes.<sup>[3]</sup> These 2D filtration materials are widely developed so far because they can realize economic oil/water separation by gravity and their separation flux is always high. The second strategy is to use oil/organic solvent adsorbent materials, such as superhydrophobic–superoleophilic sponge/foam<sup>[4]</sup> and aerogel,<sup>[5]</sup> to realize separation by absorbing oil/organic solvent while simultaneously repelling water. Some of these materials can be reused

by simply squeezing or burning after each adsorption cycle, showing high separation efficiency and applicability. These 3D adsorption materials are applicable in large-scale industrial separations because these adsorbent materials can be connected to a pump/vacuum system to achieve a high-efficiency continuous oil/organic solvent and water separation applications.<sup>[6]</sup> However, some of these materials are susceptible to corrosive

## 1. Introduction

Oils/organic solvents spills cause serious environmental issues in terms of both water contamination and oil waste, which further require a lot of energy consumption and economic burden for water remediation.<sup>[1]</sup> Recently, materials with superwettability such as superhydrophobicity and

Dr. F. Chen, Dr. X. Liu, Dr. J. Song  
Key Laboratory for Precision and Nontraditional Machining Technology  
of the Ministry of Education  
Dalian University of Technology  
Dalian 116024, P. R. China  
E-mail: xinliu@dlut.edu.cn

Dr. F. Chen, Dr. G. He, Prof. C. J. Carmalt, Prof. I. P. Parkin  
Materials Chemistry Research Centre  
Department of Chemistry  
University College London  
20 Gordon Street, London WC1H 0AJ, UK  
E-mail: i.p.parkin@ucl.ac.uk

Dr. Y. Lu, Dr. M. K. Tiwari  
Nanoengineered Systems Laboratory  
UCL Mechanical Engineering  
University College London  
London WC1E 7JE, UK

Dr. J. Song  
Collaborative Innovation Center of Major  
Machine Manufacturing in Liaoning  
Dalian University of Technology  
Dalian 116024, China

 The ORCID identification number(s) for the author(s) of this article can be found under <https://doi.org/10.1002/adfm.201702926>.

DOI: 10.1002/adfm.201702926

aqueous solutions (e.g., strong acid and alkali),<sup>[4b,d,7]</sup> which affects their separation performance in these complex environments. Therefore, it is still of great importance to develop advanced materials that can be used for continuous separation of immiscible oils/organic solvents and corrosive aqueous solutions.

Poly(vinylidene fluoride) (PVDF) is widely explored polymer to form functional films/membranes that can be used for various applications, such as oil/water separation and membrane distillation, due to its outstanding chemical resistance, biocompatibility, thermal/mechanical stability and UV tolerance.<sup>[8]</sup> For example, Zhang et al.<sup>[9]</sup> prepared superhydrophobic–superoleophilic PVDF membranes by a phase-inversion approach and ammonia-assisted dehydrofluorination, and realized effective separation of various water-in-oil emulsions. Yu et al.<sup>[10]</sup> fabricated superhydrophobic and superoleophilic porous boron nitride nanosheet/PVDF composite material by gelation and freeze-drying, and this material could be used for oil-polluted water cleanup. An et al.<sup>[11]</sup> reported a superhydrophobic PDMS–PVDF hybrid electrospun membrane, which was used for wastewater treatment. However, owing to the poor solubility of PVDF, the all hitherto reported PVDF-based materials with superwettability involved the use of toxic organic solvents, such as *N,N*-dimethylformamide (DMF), *N*-methyl-2-pyrrolidone (NMP), triethyl phosphate (TEP), and *N,N*-dimethylacetamide (DMAC);<sup>[9–12]</sup> these solvents are harmful to the operators and the environment and naturally result in volatile organics components (VOC) release, which is highly undesirable. As green chemistry and sustainable engineering have recently witnessed a significant growth of interest for water cleaning,<sup>[13]</sup> developing environmentally friendly methods to fabricate PVDF-based materials with superhydrophobicity for oil/organic solvent and water separation is of great importance.

Generally, there are two strategies for making superhydrophobic materials—either to roughen a low surface energy material or to reduce the surface energy of a highly textured surface.<sup>[14]</sup> PVDF, as a low surface energy material ( $\approx 25$  dynes  $\text{cm}^{-1}$ ) due to its repeating unit of  $-\text{CF}_2-\text{CH}_2-$ , could achieve superhydrophobicity using the former strategy.<sup>[12b]</sup> In this paper, we used table salt, an economical and water-soluble material, as a sacrificial template and multiwall carbon nanotubes (MWCNTs) to roughen the PVDF. The whole process did not use or release any organic solvents. The PVDF–MWCNT foam showed its reusability and high adsorption capacity to various oils/organic solvents even after 48 h intense UV exposure. We further demonstrated a highly stable and continuous separation of oils/organic solvents and corrosive aqueous solutions using a vacuum-assisted PVDF–MWCNT foam adsorption system in highly acidic, alkaline, and salty environments. The organic solvent-free and reusable PVDF–MWCNT foam is a promising candidate for large-scale industrial separation of oil/organic solvent and water in corrosive, turbulent, and outdoor conditions, with minimized pressure to the environment.

## 2. Results and Discussion

Porous PVDF–MWCNT foam was prepared by heating a mixture of PVDF powder, MWCNTs and table salt particles, and

then dissolving the sacrificial table salt template, as shown in **Figure 1a**. After immersing in water for 24 h, the table salt could be removed, and the porous structures were thereafter created (Figure S1, Supporting Information). The preparation was totally organic solvent free and thus environmentally friendly. The majority of the reported porous PVDF–MWCNT foam in this paper was fabricated with the mass ratio of  $m_{\text{PVDF}}:m_{\text{table salt}}:m_{\text{MWCNT}} = 1:7:0.1$ , unless specified otherwise. Figure 1b shows a picture of the as-prepared porous PVDF–MWCNT foam, and its surface morphology is shown in Figure 1c,d. The SEM image in Figure 1c shows that the foam consists of PVDF–MWCNT skeletons and irregular pores, forming a porous, interconnected 3D framework. Figure 1d clearly demonstrates that the added MWCNTs obviously roughened the foam surface by forming some submicron structures. The bulk density of the PVDF–MWCNT foam was about  $0.197 \text{ g cm}^{-3}$ , and the porosity was calculated to be  $\approx 89\%$ . Notably, no apparent difference in the morphology or pore was observed between the top surface and the inside of the foam (Figure S2, Supporting Information). The attenuated total reflectance Fourier transform infrared spectroscopy (ATR–FTIR) spectrum of the PVDF–MWCNT foam is depicted in Figure S3a (Supporting Information). The bands at 761, 792, and  $972 \text{ cm}^{-1}$  were attributed to the  $\alpha$  phases of PVDF, while the bands at 840 and  $1211 \text{ cm}^{-1}$  were assigned to the  $\beta$  phases.<sup>[15]</sup> The absorption bands at  $1400$  and  $1379 \text{ cm}^{-1}$  were associated with the deformation vibration of  $-\text{CH}_2$ , the stretching vibration of  $-\text{CF}_2$  could be found at  $1147$  and  $1180 \text{ cm}^{-1}$ , and the characteristic peak at  $870 \text{ cm}^{-1}$  was assigned to the skeletal vibration of PVDF C–C bonds.<sup>[16]</sup> XRD patterns also confirmed the existence of  $\alpha$  (Miller indices of (020) and (110)) and  $\beta$  (Miller indices of (110)) phases of PVDF (Figure S3b, Supporting Information).<sup>[17]</sup> XPS spectra of the pure PVDF and the PVDF–MWCNT foam demonstrated that the atomic content of C increased from 51.34 to 56.93 at% after the introduction of MWCNTs (Figure S3c, Supporting Information). The high resolution C 1s peaks of pure PVDF was characterized by three peaks of  $-\text{CH}/\text{C}-\text{C}$  at 284.6 eV,  $-\text{CH}_2$  at 286.8 eV and  $-\text{CF}_2$  at 291.1 eV,<sup>[18]</sup> and for the PVDF–MWCNT foam, the intensity of peak at 284.6 eV obviously increased, which could be attributed to the  $\text{sp}^2 \text{ C}=\text{C}/\text{sp}^3 \text{ C}-\text{C}$  from the MWCNTs (Figure S3d, Supporting Information).<sup>[19]</sup> Additionally, we also note that the heat treatment at  $200^\circ \text{C}$  for 30 min did not cause obvious dehydrofluorination or crosslinking among the polymer chains, because the atomic ratio of F/C remained almost the same before and after heat treatment (Figure S4, Supporting Information).

As shown in Figure 1b,e, the water droplets on the foam surface beading up and the resulting water contact angle was measured to be  $152.5 \pm 4.5^\circ$ , showing good water repellence, while a toluene droplet deposited on the foam was adsorbed quickly and the oil/organic solvent contact angle was  $\approx 0^\circ$ . When the porous foam was immersed in water, a shiny and reflective water–foam interface could be clearly seen, as shown in Figure 1f and Video S1 (Supporting Information), because of the presence of a trapped air layer within the porous structure. When water droplets were dropped onto the inclined PVDF–MWCNT foam surface, they easily bounce away without any adhesion (Figure 1g). Moreover, the porous foam exhibited a structural flexibility, as shown in Figure 1h and Video S2

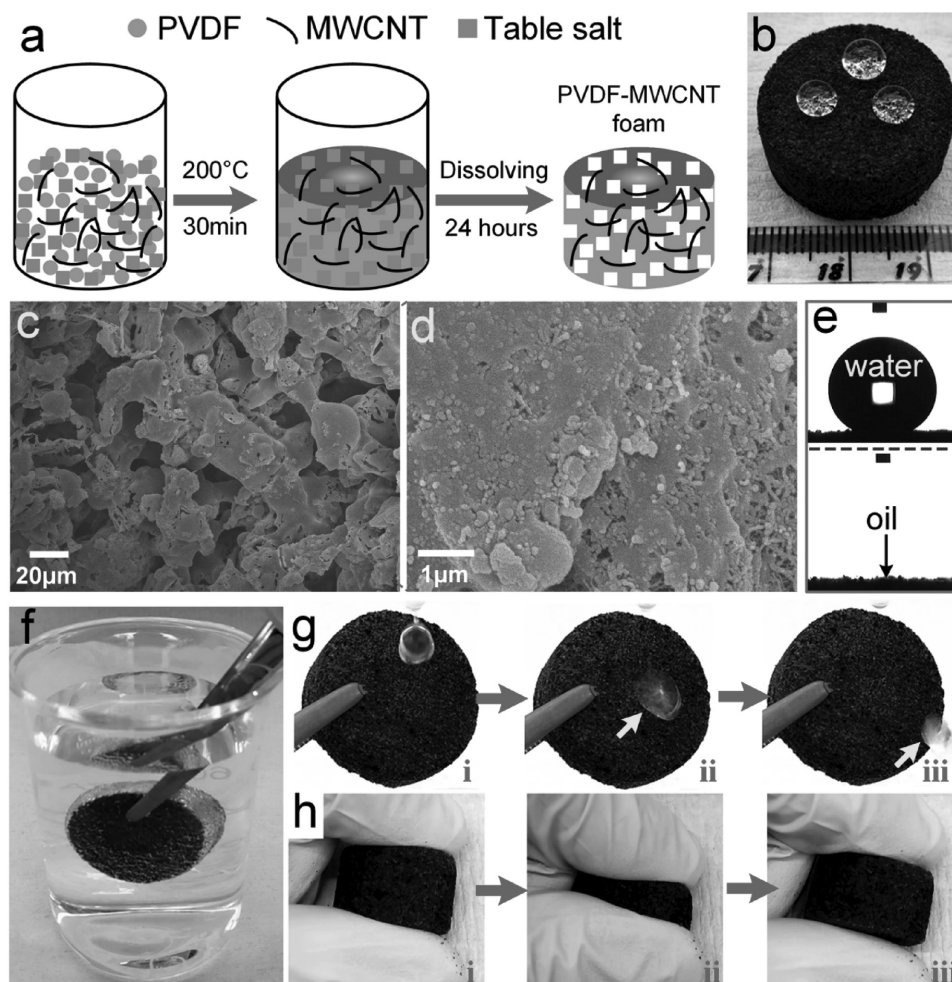


**Figure 1.** a) Illustration of the facile fabrication of porous PVDF–MWCNT foam. b) Picture of as-prepared porous PVDF–MWCNT foam ( $m_{\text{PVDF}}:m_{\text{table salt}}:m_{\text{MWCNT}} = 1:7:0.1$ ), with water droplets on top. c, d) The SEM images of the porous PVDF–MWCNT foam with different magnifications. e) Optical images of water and toluene droplets deposited on the foam. f) Photograph of the foam immersed in water showing a shiny liquid water–foam interface, which revealed the presence of trapped air layer on the foam surface. g) Image sequence capturing a water droplet easily bouncing away after hitting the superhydrophobic foam (as pointed by the yellow arrows). h) Image sequence showing (i,ii) manual compression to over 50% and (iii) near complete recovery to its original shape after release.

(Supporting Information). The PVDF–MWCNT foam could almost recover to its original shape without losing its antiwetting property after manual compression of about 50%. After being repeatedly compressed for 10 cycles, about 90% of its initial thickness was maintained (Figure S5, Supporting Information), revealing its good springiness that can be beneficial in reusing the porous foam for oils/organic solvents adsorption and collecting the adsorbed oils/organic solvents.

The influence of mass ratio of the raw materials (PVDF, MWCNT, and table salt) on water contact angle of the foam was then evaluated. By fixing the content of MWCNT at 10% of PVDF, the influence of mass ratio between PVDF and table salt on the water contact angle was firstly studied, and the results are depicted in Figure 2a. The water contact angle increased from  $137.7 \pm 10.8^\circ$  to  $151.9 \pm 5.0^\circ$  with the  $m_{\text{PVDF}}:m_{\text{table salt}}$  ratios of 1:1 to 1:5, and then remained above  $150^\circ$  with further rise in the table salt content. The water contact angle of the foam prepared from different ratios of MWCNT with

respect to PVDF while keeping  $m_{\text{PVDF}}:m_{\text{table salt}} = 1:7$  was investigated and shown in Figure 2b. MWCNT played a key role in making the foams superhydrophobic. The water contact angle was  $122.2 \pm 7.8^\circ$  for the porous foam without MWCNT, and the water droplets placed on it would easily get stuck due to the skeleton of the PVDF foam surface was relatively smooth (Figure S6, Supporting Information). The water contact angle increased to  $152.6 \pm 4.5^\circ$  when the MWCNT content was 10%; further rise of MWCNT content had little effect on the contact angle. Superhydrophobicity is extremely important for the foam to realize selective adsorption of oil/organic solvent, especially when heavy oil/organic solvent deposits under aqueous solution. In this case, superhydrophobic PVDF–MWCNT foam will stop aqueous solution from penetrating.

Adsorption capacity, defined as the mass ratio of the adsorbed oil compared to the foam itself when the foam was oil-saturated, was an important parameter to evaluate the oil/water separation performance of the foam. For porous

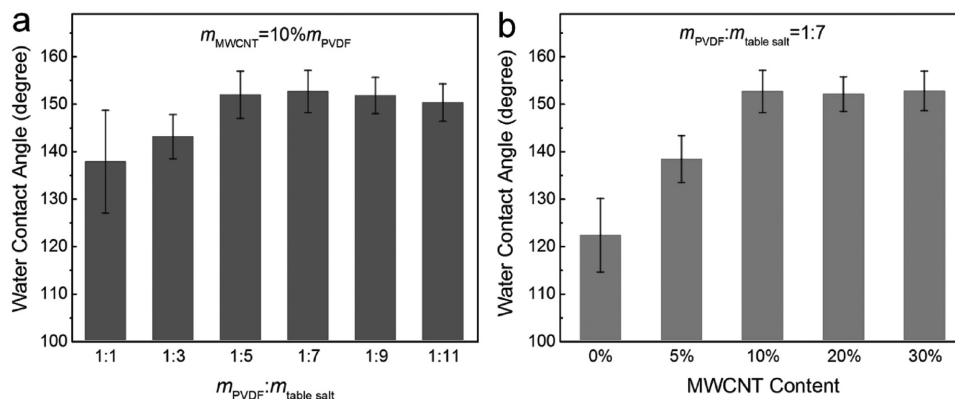


**Figure 2.** a) The influence of mass ratio of PVDF to table salt (the mass ratio of MWCNT to PVDF was kept at 10%) on water contact angle of the foam. b) The influence of MWCNT content with respect to PVDF on water contact angle of the foam by fixing  $m_{\text{PVDF}}:m_{\text{table salt}} = 1:7$ .

oil/organic solvent adsorbents, porosity is crucial to their adsorption capacity. By fixing the content of MWCNT at 10% of PVDF, the influence of mass ratio between PVDF and table salt on the porosity of the porous foam was studied, and the results are depicted in **Figure 3a**. The mass ratio has a great effect on the observed porosity. As the  $m_{\text{PVDF}}:m_{\text{table salt}}$  changed

from 1:1 to 1:7, the porosity increased from 76.5% to 88.9%. The porosity further increased to 92.5% when the ratio was 1:11, but the foam was then too fragile and easily crumbled by compression (Figure S7, Supporting Information). Figure 3b shows that the toluene adsorption capacity was only  $166.2 \pm 8.9\%$  when  $m_{\text{PVDF}}:m_{\text{table salt}} = 1:1$ , but improved as the

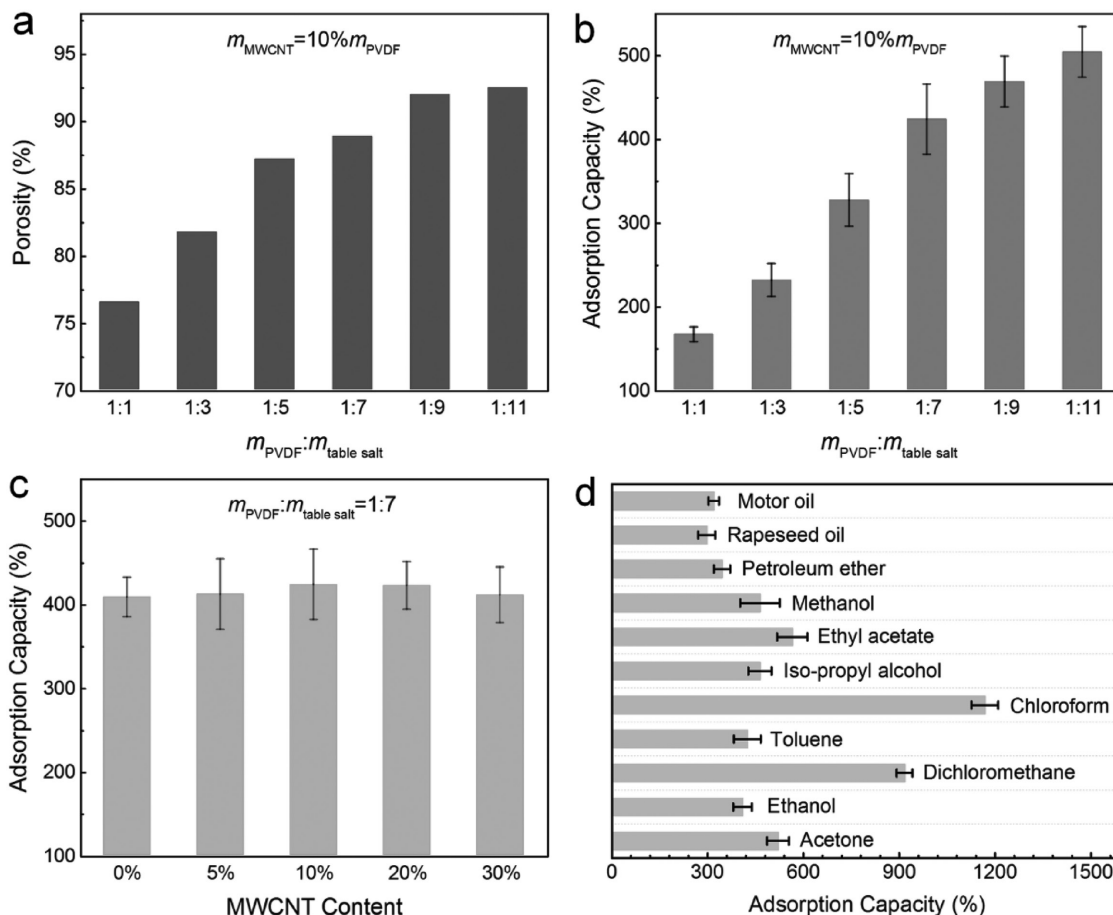


**Figure 3.** The influence of mass ratio of PVDF to table salt ( $m_{\text{MWCNT}} = 10\% m_{\text{PVDF}}$ ) on a) porosity and b) toluene adsorption capacity of the foam. c) The influence of MWCNT content with respect to PVDF on toluene adsorption capacity of the foam ( $m_{\text{PVDF}}:m_{\text{table salt}} = 1:7$ ). d) Adsorption capacity of the PVDF–MWCNT foam ( $m_{\text{PVDF}}:m_{\text{table salt}}:m_{\text{MWCNT}} = 1:7:0.1$ ) toward different oils/organic solvents.



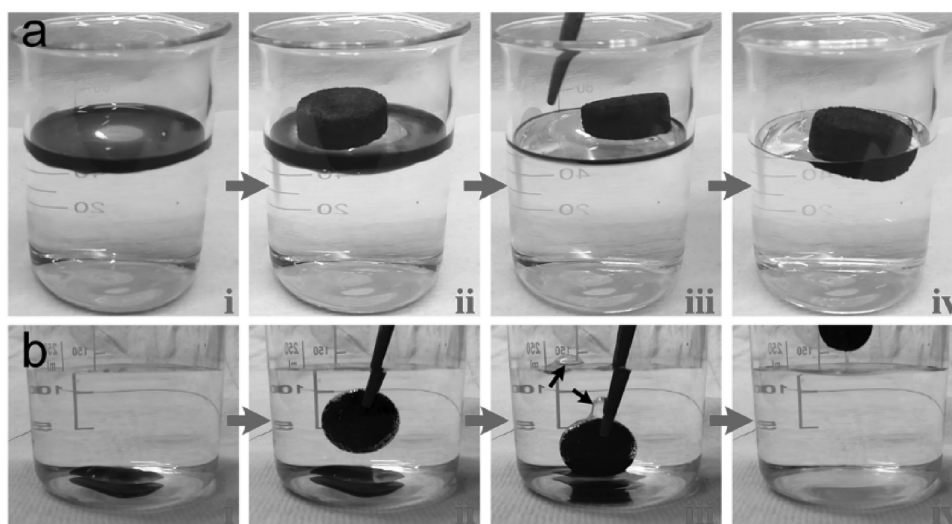
table salt content increased in the initial synthesis, and reached  $504.2 \pm 30.4\%$  when the ratio was 1:11. Next, the porosity and toluene adsorption capacity of the foam prepared from different ratios of MWCNT with respect to PVDF while keeping  $m_{\text{PVDF}}:m_{\text{table salt}} = 1:7$  was investigated. We found that the mass content of MWCNT herein had little effect on the porosity of the prepared foam. Additionally, there is no obvious toluene adsorption capacity change was found when increasing MWCNT content from 0% to 30% (Figure 3c), demonstrating that the MWCNT had little influence on oil/organic solvent adsorption capacity of the foam. However, addition of too much MWCNT could obviously weaken the robustness of the foam, as the foam could be easily destroyed and obvious materials shedding even could be seen when touching the foam by hand (Figure S8, Supporting Information).

Figure 3d presents the adsorption capacity of the porous PVDF–MWCNT foam toward different oils/organic solvents. It can be seen that the adsorption capacities of the foam for the various tested oils/organic solvents are in the range of  $\approx 300\%$  to  $\approx 1200\%$ . Generally, the adsorption capacity of adsorbents was affected by the density and viscosity of oils/organic solvents.<sup>[20]</sup> For oils/organic solvents with low viscosity, including ethanol, petroleum ether, methanol, ethyl acetate, isopropyl alcohol, chloroform, toluene, dichloromethane and acetone, the adsorption capacities were basically proportionate to their densities (Table S1, Supporting Information). However, oils/organic solvents with high viscosity (e.g., rapeseed oil and motor oil, Table S1, Supporting Information) tended to block the pores of the porous foam when being adsorbed because of the slow diffusion speed, which further locked air inside the porous foam and thus resulted in a low adsorption capacity ( $297.0 \pm 26.7\%$  for rapeseed oil and  $319.1 \pm 16.4\%$  for motor oil). However, the adsorption capacity obtained under atmosphere could be improved by vacuum-assisted oil/organic solvent adsorption. For example, when rapeseed oil and motor oil adsorptions were

conducted under vacuum ( $\approx 5.0$  kPa) for 10 min, the adsorption capacity respectively increased to  $\approx 540\%$  and  $\approx 510\%$ .

Selective adsorptions tests were conducted using both light and heavy organic solvents to demonstrate the separation ability of the porous foam toward oil/organic solvent and water mixtures. Figure 4a and Video S3 (Supporting Information) show an example of light organic solvent removal from water surface, in which blue dyed toluene (8 mL) was set as the exemplar oil and dispersed on water surface. After placing a porous PVDF–MWCNT foam ( $\approx 0.487$  g) on the water spills, the toluene could be completely adsorbed in less than 20 s, showing an efficient water spill clean-up ability. Figure 4b and Video S4 (Supporting Information) show the heavy organic solvent removal from underneath water. As can be seen, when the foam was immersed in water, a mirror surface appeared because of the trapped air which was then driven out after the foam contacted with the predeposited chloroform (dyed with oil red). No residual chloroform was observed after clean-up, demonstrating the excellent selective separation ability of the porous foam underwater. Notably, when the thickness of the 3D PVDF–MWCNT foam was well regulated, quasi-2D PVDF–MWCNT filtration could be created for oil/water separation. As shown in Figure S9 and Video S5 (Supporting Information), a PVDF–MWCNT filtration with thickness of  $\approx 3$  mm was prepared to realize gravity-driven chloroform/water separation, demonstrating the versatility of the proposed template dissolving method for preparing advanced oil/water separation materials.

Reusability is very important for those oil/organic solvent adsorbents considering the adsorption efficiency and cost. Some general methods, including combustion,<sup>[5b,21]</sup> mechanically squeezing,<sup>[4c,5b,22]</sup> evaporation by heating,<sup>[5c,21a,23]</sup> and release in other solvent,<sup>[24]</sup> were employed to reuse the oil/organic solvent adsorbents. The combustion method can refresh the adsorbents easily, but it is only appropriate for



**Figure 4.** Light and heavy oils/organic solvents and water separation using the porous PVDF–MWCNT foam. a) Removal of toluene (light organic solvent) on water surface by the foam: (i) the mixture of toluene (dyed with oil blue) and water, (ii–iv) the adsorption was completed within 18 s after a the foam was dropped in. b) Selective adsorption of chloroform (heavy organic solvent) under water: (i) the mixture of chloroform (dyed with oil red) and water, (ii) the foam was immersed in water, showing a mirror surface due to the trapped air, (iii) chloroform was quickly adsorbed when contacted with the foam, and the air inside the porous foam was driven out as pointed by the black arrows, (iv) no residual chloroform could be observed after clean-up.

flammable oils/organic solvents and heat-resistant adsorbents, and the adsorbed oils/organic solvents cannot be recycled and reused, so this method is neither economical nor environment friendly. For adsorbents with flexibility, the squeezing method is a primary way for reusability as it is quick and simple to perform, though the adsorption capacity may slightly decrease after the first cycle because the adsorbed oil/organic solvent is unlikely to be completely squeezed out. Evaporation by heating is feasible for thorough removal of highly volatile oils/organic solvents, and the evaporated oils/organic solvents can also be easily collected (i.e., distillation) for recycle. Comparatively, releasing in other solvents (e.g., ethanol) could be an excellent tool to completely remove high viscosity or nonvolatile oils/organic solvents from the adsorbents, and the adsorbents can be further reused for oils/organic solvents adsorption just after drying. Here, three methods were employed to reuse the porous PVDF–MWCNT foam, as shown in Figure 5, and the masses before (remnant mass) and after adsorption (adsorbed mass) of each cycle were recorded to evaluate its adsorption capacity. First, a heating method was employed to reuse the porous foam for easily volatile organic solvent. As shown in Figure 5a, the foam ( $\approx 0.366$  g) was heated after toluene adsorption at  $120\text{ }^\circ\text{C}$  for 20 min, and no obvious change in adsorption capacity was found during 10 adsorption/heating cycles,

with an average adsorbed mass remained at  $1.916 \pm 0.025$  g indicating an adsorption capacity of  $420.7 \pm 8.1\%$ . Second, for the reusing of the foam used for oils/organic solvents with high viscosity, releasing in ethanol and drying at  $90\text{ }^\circ\text{C}$  for 10 min was applied. As shown in Figure 5b, a porous PVDF–MWCNT foam (0.538 g) was used to adsorb motor oil, and the mass after adsorption during 10 cycles remained at  $2.292 \pm 0.031$  g (the corresponding adsorption capacity was about  $322.9 \pm 5.1\%$ ), showing potential for excellent reusability of high viscosity oils/organic solvents using the foams developed herein. Finally, the squeezing method was employed to demonstrate the reusability of the foam because of its good elasticity (c.f. Figure 1h above). As shown in Figure 5c, the mass of the sponge-like foam increased from 0.549 to 2.787 g after the first cycle of toluene adsorption, showing an adsorption capacity of 407.7%. During the following nine cycles, the remnant mass stabilized at about  $0.890 \pm 0.041$  g because the adsorbed toluene could not be totally squeezed out. Though the adsorbed mass of the second cycle decreased to 2.435 g because of the slightly collapsed pores induced by compression, the adsorbed mass in the following eight cycles was above 2.2 g (i.e., adsorption capacity of 300%), demonstrating the good reusability of the foam and potential for recycling the adsorbed oils/organic solvents by a squeezing method. As an illustration, Figure 5d and

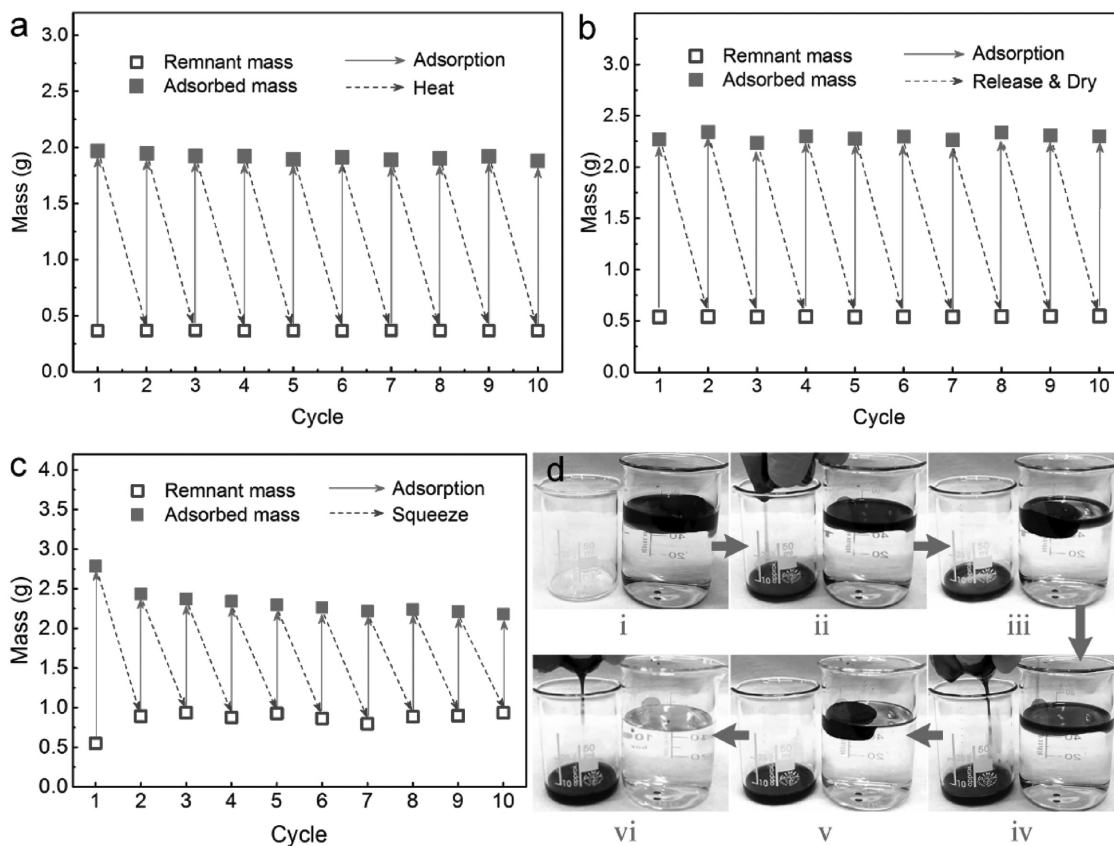


**Figure 5.** Three methods to reuse the as-prepared porous PVDF–MWCNT foam. a) The reusability of the foam for toluene recovery using heating method. b) Reusing the foam for absorption of motor oil by releasing in ethanol & drying. c) The reusability of the foam using the direct squeezing method. d) Image sequence demonstrating the reuse by squeezing to clean up spilled toluene (dyed with oil blue) on water: the first (i,ii), second (iii,iv) and third (v,vi) cycle of adsorption/squeezing.

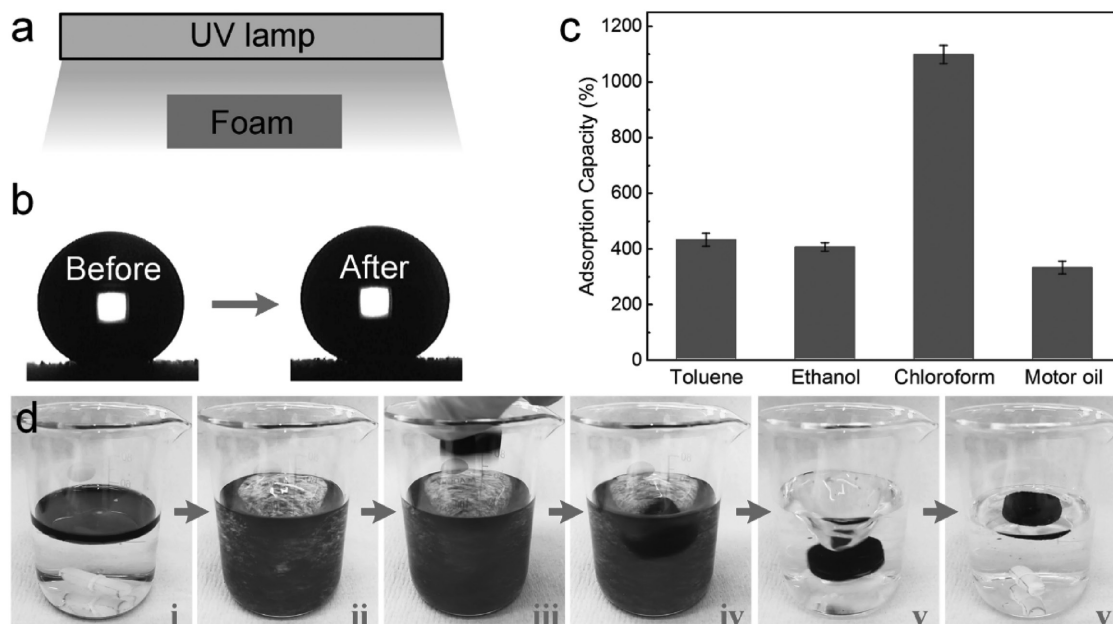


**Figure 6.** Durability and usability of the PVDF–MWCNT foam under complex outdoor environments. a) The schematic diagram of UV irradiation. b) Optical images of water droplet on the foam before and after 48 h UV exposure. c) Oil/organic solvent adsorption capacity of the foam after 48 h UV irradiation. d) Image sequence showing toluene removal from water under strong stirring: (i) the toluene/water mixture, (ii) the mixture under strong stirring ( $\approx 400 \text{ r min}^{-1}$ ), (iii) a PVDF–MWCNT foam dropped into the mixture, (iv–vi) the toluene adsorption is completed within 15 s.

Video S6 (Supporting Information) show a three-cycle adsorption-squeezing process to remove toluene from water surface by using our porous PVDF–MWCNT foam.

In practical immiscible oils/organic solvents and aqueous solutions separations, the working environment could be extremely harsh, such as intensive UV radiation in outdoor exposure, high acidity or basicity of industrial oily wastewater, and high salt concentration of seawater. Separation environments can also involve flow complexity and turbulence, which pose additional challenge on mechanical stability and separation efficacy. Therefore, the separation ability of the adsorbents in these complex environments is important to be investigated. **Figure 6a** shows the schematic diagram of UV irradiation of the PVDF–MWCNT foam. 48 h intense UV exposure had little influence on the water repellence of the foam, as shown in **Figure 6b**. The oils/organic solvents adsorption capacities of the foam after UV exposure were measured and depicted in **Figure 6c**, we can clearly see that the adsorption capacities were almost the same with the values before UV irradiation (**Figure 3d**), demonstrating excellent oil/organic solvent removal ability in outdoor applications. Then a highly turbulent oil/organic solvent and water mixture was simulated by strong magnetic stirring ( $\approx 400 \text{ r min}^{-1}$ ), and **Figure 6d** displays the image sequence of toluene removal from such a mixture under strong stirring (**Video S7**, Supporting Information), the toluene removal could be completed within 15 s, showing efficient oil/organic solvent and water separation under highly turbulent environment.

Moreover, the porous PVDF–MWCNT foam showed superhydrophobicity toward droplets of HCl, NaOH, and saturated NaCl, and it also retained superhydrophobicity after being immersed in these solutions for 24 h, as illustrated in **Figure 7a**,

showing excellent durability against acidic, alkaline, and saline solutions. **Figure 7a** also depicts the oil removal percentage of the foam from the mixtures of motor oil, respectively with HCl, NaOH, and saturated NaCl solution. The results show that more than 99% of the added motor oil could be separated by the foam in highly acidic, alkaline and salty environments. Notably, when the foam was put into these pure solutions (i.e., no oil was added) for 10 min, no obvious mass change was observed after withdrawal. The ATR–FTIR spectra of the separated motor oils were dominated by characteristic vibrations of carbon-related functional groups, while no band assigned to water could be observed, confirming the high purity of the separated oils (**Figure S10a–c**, Supporting Information).<sup>[25]</sup>

Additionally, to further demonstrate its potential in practical large scale oil/organic solvent spills separation from aqueous solutions (especially under complex environments), vacuum-assisted continuous oil/organic solvent collecting in acidic, alkaline, and salty environments were investigated, and the schematic diagram of the separation is depicted in **Figure 7b**. The foam was attached to a pipe and then connected to an oil/organic solvent “tank” which was connected to a vacuum pump system. When the foam was exposed to immiscible oil/organic solvent and aqueous solution mixture, oil/organic solvent could be quickly adsorbed and filled the pores of the porous foam while aqueous solution was repelled due to the superhydrophobicity and superoleophilicity. Then the adsorbed oil/organic solvent blocked the air channels in the porous foam, which allowed the vacuum pump system to provide a force to suck the oil/organic solvent into the “tank,” and when the oil/organic solvent was completely removed, the air channels in the porous foam regenerated and thus avoided the suction of aqueous solution into the porous foam.<sup>[6,13b]</sup> With the assistance of a

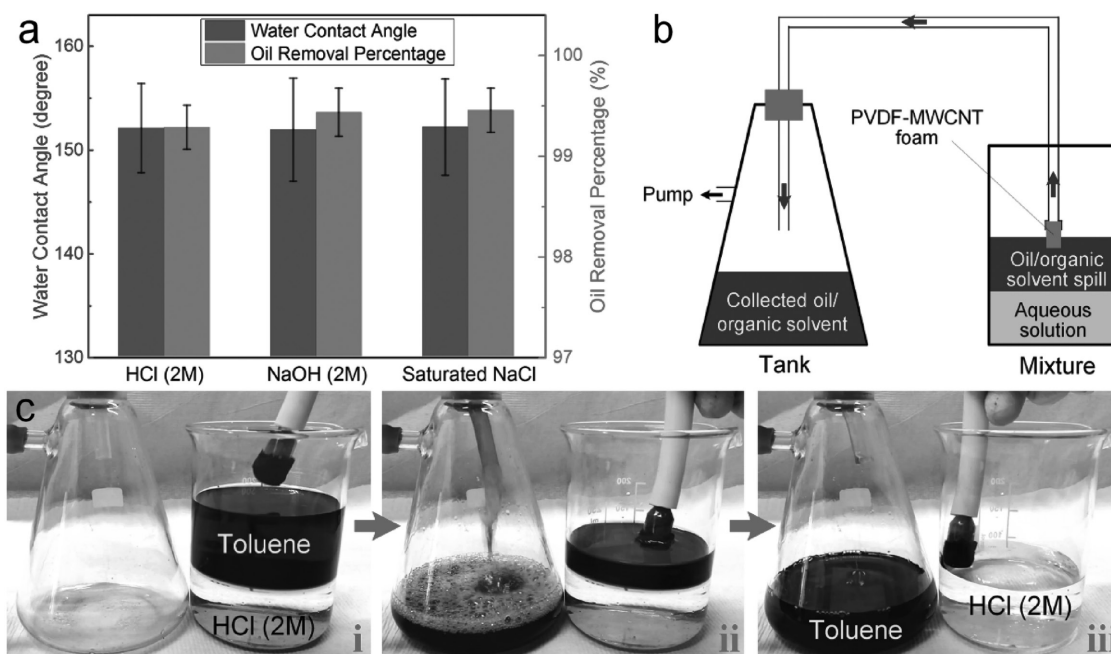


**Figure 7.** a) The water contact angle of the PVDF–MWCNT foam after being immersed in HCl (2 M), NaOH (2 M), and saturated NaCl ( $\approx 26.5\%$ ) solution for 24 h, and the oil removal percentage in terms of their mixtures with motor oil. b) The schematic diagram of vacuum-assisted continuous oil/organic solvent and aqueous solution separation. c) Digital photograph showing the vacuum-assisted continuous separation of toluene/HCl (2 M) mixture.

pump, oil/organic solvent removal ability of the adsorbents can be independent of its original adsorption capacity, which greatly improves the separation efficiency and decreases the amount of adsorbents required. Therefore, pump-assisted continuous oil/organic solvent collection by porous adsorbents could be desirable for large scale oil/organic solvent and aqueous solution separations.<sup>[6,13b]</sup> Figure 7c and Video S8 (Supporting Information) depict the vacuum-assisted continuous collection of toluene (dyed with oil blue) from strongly acidic solution (HCl, 2 M) surface. By applying a vacuum pressure of  $\approx 2.2$  kPa for about 1 min, the toluene was totally separated from the mixture. No water was observed to be in the collected toluene, which was also confirmed by ATR–FTIR spectra of the collected toluene (Figure S10d, Supporting Information), demonstrating a quick and efficient oil/organic solvent separation from corrosive acid solution under vacuum assistance. Similarly, the porous PVDF–MWCNT foam could be used for the continuous separation of oil/organic solvent mixed with highly alkaline (NaOH, 2 M, Figure S11a and Video S9, Supporting Information) or salty (saturated NaCl,  $\approx 26.5\%$ , Figure S11b and Video S10, Supporting Information) solutions. Therefore, the proposed porous PVDF–MWCNT foam seems to have clear potential for practical applications.

Finally, we also compared the performance of the foam presented herein against those from the recent literatures (Table S3, Supporting Information). Among those reported, carbon-based ultralight adsorbents, such as carbon nanotube (CNT) sponge,<sup>[4a]</sup> pyrolyzed melamine/lignin sponge,<sup>[26]</sup> carbon aerogel,<sup>[27]</sup> and cellulose aerogel,<sup>[13c]</sup> are characterized with ultrahigh oil/organic solvent adsorption capacity (up to  $\approx 30\,000\%$ ), but their preparation processes are either complex/inefficient or harmful to the environment/operator, and their

oil/organic solvent removal stability in highly acidic, alkaline, and salty environments have rarely been considered. Functionalized commercial sponges, such as polyurethane sponge coated with Ag,<sup>[4b]</sup> CNT,<sup>[7a]</sup> nanodiamonds,<sup>[7b]</sup> straw soot,<sup>[7c]</sup> and iron oxide/polytetrafluoroethylene particles<sup>[4f]</sup> and melamine sponge coated by polydopamine particles,<sup>[4d]</sup> are the most explored materials for oil/organic solvent selective adsorption due to their inherently 3D porous structures and low density. The adsorption capacities of these materials are also impressive (up to  $\approx 4500\%$ ), but their functionalization process always involves chemical reactions (e.g., chemical etching, deposition, and modification), which goes against the concept of green and sustainable engineering. Additionally, though these functionalized materials are chemically stable, they partly or even completely lose their water repellence when being exposed to strong acids or bases,<sup>[4b,d,7]</sup> which could be attributed to the poor chemical stability of the polymeric sponge itself. By contrast, a porous boron nitride nanosheet (BNNS)–PVDF composite material reported by Yu et al.<sup>[10]</sup> showed excellent chemical resistance toward liquids with a wide pH range (0 to 14) due to the chemical stability of both BNNS and PVDF. However, the toxic organic solvent, DMF, was required for its fabrication. Sponges consisting of PDMS,<sup>[20,22,28]</sup> PDMS–graphene,<sup>[29]</sup> and PDMS–MWCNT<sup>[24c]</sup> fabricated by the sacrificial template dissolving method show lower adsorption capacities compared with most of the above mentioned adsorbents, but the preparation process is very simple and ecofriendly. The porous PVDF–MWCNT foam presented in this paper shows similar oil/organic solvent adsorption capacity with these PDMS-based sponges, and it could be easily reused by simple squeezing, heating or releasing in ethanol many times. More importantly, the chemical stability of the prepared PVDF–MWCNT foam



toward strongly acidic, alkaline, and salty solutions was demonstrated to be excellent. Therefore, as an environmentally friendly, chemically stable, and highly reusable absorbent, the PVDF–MWCNT foam could be an excellent candidate for the large scale separation of immiscible oil/organic solvent and aqueous solution mixtures.

### 3. Conclusion

In summary, we used table salt as a sacrificial template to fabricate porous PVDF–MWCNT foam with superhydrophobicity and superoleophilicity, the fabrication process was totally organic solvent free. The prepared porous foam could be easily compressed to more than 50%, and almost fully recovered after release. The oil/organic solvent adsorption capacity of the prepared porous foam was as high as 300–1200% of its own weight depending on the density and viscosity of the oils/organic solvents. The porous oil/organic solvent adsorbent could be easily reused by squeezing, heating, or releasing in other solvents for more than 10 cycles without an obvious decrease in adsorption capacity. Owing to the excellent chemical stability of PVDF and MWCNT, the superhydrophobicity of the prepared foam showed remarkable durability in highly acidic, alkaline and salty environments, and the oil/organic solvent removal percentage in these complex environments was demonstrated to be more than 99%. Pump-assisted continuous separation of oil/organic solvent and corrosive aqueous solutions was successfully demonstrated, establishing potential exploitation of the presented foam in large-scale oil/organic solvent clean-up. The foam possessed excellent UV resistance, which could be of great importance for long-term outdoor applications. Additionally, oil/organic solvent separation from mixtures under highly turbulent conditions was also realized. The proposed method to prepare the porous PVDF foam is organic-solvent free and relatively environmentally friendly, can be generalized to various PVDF-based functional materials to suit a variety of different practical exploitations.

### 4. Experimental Section

**Materials:** PVDF powder ( $M_w \approx 534\,000$ , density  $\approx 1.74\text{ g cm}^{-3}$ ) and MWCNTs (outer diameter of  $10 \pm 1\text{ nm}$ , inner diameter of  $4.5 \pm 0.5\text{ nm}$  and length of  $3\text{--}6\text{ }\mu\text{m}$ , density  $\approx 2.1\text{ g cm}^{-3}$ ) were bought from Sigma-Aldrich, UK. Organic solvents, including ethanol, petroleum ether, methanol, ethyl acetate, isopropyl alcohol, chloroform, toluene, dichloromethane, and acetone were purchased from Fisher Scientific UK and used as supplied. Motor oil (FORMULA 1 20W50) was obtained from Tetrosyl Limited (Bury, Lancashire, UK). Rapeseed oil was produced by KTC (Edibles) Ltd. (UK). Table salt was purchased from Wm Morrison Supermarkets PLC (London, UK). The basic parameters of various oils/organic solvents used in the experiments are list in Table S1 (Supporting Information).

**Fabrication of Porous PVDF–MWCNT Foam:** PVDF, table salt, and MWCNT with different mass ratios were mixed and mechanically ground to form a uniform powder. Table salt was used to create the porous structures of the foam, and MWCNTs were introduced to create micro/nanometer-scale roughness and lower the surface energy. Then the mixture was poured into silica boats and heated at  $200\text{ }^\circ\text{C}$  for 30 min (Figure 1a). After cooling to room temperature, the composite

sample block was taken out and the outermost layer was removed by sandpaper. Note the hydrophobicity of PVDF enabled simple removal of the samples from the silica boats, without need for any delaminating paster. Then the samples were immersed in hot water ( $\approx 90\text{ }^\circ\text{C}$ ) that was renewed every 2 h for 24 h to completely remove the table salt to obtain the porous PVDF–MWCNT foam. Foam with various shapes could be easily obtained by using different silica boats or cutting the as-prepared samples. The porosity ( $P$ ) of the porous foam was estimated by the following equation

$$P = \frac{V_{\text{PVDF} + \text{MWCNT}}}{V_{\text{foam}}} \times 100\% \quad (1)$$

where  $V_{\text{PVDF} + \text{MWCNT}}$  and  $V_{\text{foam}}$  are the real volume of used raw materials (PVDF and MWCNT) and the macroscopic volume of the foam, respectively.  $V_{\text{PVDF} + \text{MWCNT}}$  can be obtained from the mass and density of PVDF and MWCNT while  $V_{\text{foam}}$  can be calculated directly from the size of the foam.

**Sample Characterization:** Contact angles measurements of water and organic solvents were performed by an optical contact angle meter (FTA 1000) at room temperature with droplets of  $\approx 5\text{ }\mu\text{L}$ . At least six different positions on each sample were tested. The surface morphologies of the samples were observed by scanning electron microscope (SEM, JEOL JSM-6700F, Japan) equipped with an energy-dispersive X-ray (EDX) spectrometer, and a layer of gold and carbon were deposited on the samples under vacuum for SEM and EDX scanning, respectively. The surface chemistries were characterized by ATR–FTIR (BRUKER) and X-ray photoelectron spectroscopy (XPS, Thermo Scientific K- $\alpha$  photoelectron spectrometer, the C 1s peak at  $284.6\text{ eV}$  was used as reference). X-ray diffraction (XRD) patterns were recorded using a STOE SEIFERT diffractometer with Mo K $\alpha$  radiation ( $\lambda = 0.709\text{ \AA}$ ).

**Oil/Organic Solvent Adsorption Capacity of the Foam:** To test oil/organic solvents adsorption capacity ( $M$ ), the porous PVDF–MWCNT foam was immersed in various oil/organic solvents at room temperature for  $\approx 10\text{ min}$  and then took out for weight measurements. The adsorption capacity ( $M$ ) was evaluated by using the following equation

$$M = \left( \frac{m}{m_0} - 1 \right) \times 100\% \quad (2)$$

where  $m_0$  and  $m$  are the weight of the foam before and after adsorption, respectively. To avoid the evaporation of highly volatile organic solvents, weight measurements were performed immediately after withdrawal and no dripping was observed on the foam. Obvious oil dripping was observed on the foam soaked by oil with high-viscosity (i.e., rapeseed oil and motor oil), so a 5 min interval and a filter paper wipe was performed before weighing. At least five measurements were conducted for each oil/organic solvent, and the average value was presented here.

**Separation of Immiscible Oils/Organic Solvents and Water:** To demonstrate the selective adsorption ability of the foam toward the mixture of immiscible organic solvent and water, toluene (light organic solvent) and chloroform (heavy organic solvent) were respectively mixed with water, and then the foams were used to selectively adsorb the organic solvents. For the toluene and water mixture, the foam was float freely on the mixture, and the dispersed toluene was removed by moving the foam. For the chloroform and water mixture, the foam was manually immersed underneath the water to contact with the chloroform and thus adsorb it.

**Reusability of the Foam:** Repeated absorption/desorption cycles of oil/organic solvents were performed to evaluate the reusability of the foam and three methods were employed to reuse the porous foam. The first method was heating the soaked foams up to a temperature that was slightly beyond the boiling point of the organic solvent (toluene). The second method was immersing the foam in ethanol to release the adsorbed oil (motor oil) and then drying at  $90\text{ }^\circ\text{C}$  for 10 min. The third method was squeezing, by which the adsorbed organic solvent (toluene) could be partly pressed out thus to recover its adsorption ability. For all

the methods, the mass of the porous PVDF–MWCNT foam before and after adsorption were recorded to evaluate its adsorption capacity.

**Durability and Oil/Organic Solvent Removal Ability of the Foam in Complex Environments:** Direct UV irradiation from  $2 \times 8$  W 365 nm UV lamp (Uvitec, Cambridge, UK) was used to simulate outdoor UV exposure, and the prepared PVDF–MWCNT foam was exposed for 48 h. Then the water contact angles and oil (toluene, ethanol, chloroform and motor oil were used as examples) adsorption capacities were measured to evaluate UV resistance. To test the oil/organic solvent removal ability of the foam in highly turbulent water, toluene/water mixture was intensely stirred under magnetic assistance ( $\approx 400$  r min<sup>-1</sup>), and then the prepared foam was dropped in to realize the selective adsorption.

Concentrated HCl (2 M), NaOH (2 M), and saturated NaCl solution ( $\approx 26.5\%$  by weight) were employed as the corrosive aqueous solutions here to evaluate the durability of the prepared porous PVDF–MWCNT foam in highly acidic, alkaline, and salty environments. After the foams were immersed in these corrosive aqueous solutions for 24 h, the water contact angles were then measured to evaluate their chemical stabilities. Additionally, slightly volatile motor oil was selected as the spill to evaluate the selective oil/organic solvent removal ability of the foam in the corrosive aqueous solutions, through which the mass error resulted from oil/organic solvent evaporation can be neglected. Motor oil (3 g) was, respectively, added into the corrosive aqueous solutions (30 g), and the oil removal by the foam (1.7 g) was processed for 10 min. Then the soaked foam was removed, and the oil removal percentage (R) was obtained according to

$$R = \left(1 - \frac{m_M - m_W}{m_O}\right) \times 100\% \quad (3)$$

where  $m_W$  and  $m_M$  are, respectively, the mass of testing solutions before and after oil removal,  $m_O$  is the mass of added motor oil. Motor oil removal from its mixture with each corrosive aqueous solution was conducted for five times, and the average value of R was reported here.

**Continuous Separation of Oils/Organic Solvents and Corrosive Aqueous Solutions:** To achieve a continuous separation of immiscible oil/organic solvent and aqueous solution, especially in highly acidic, alkaline and salty environments, vacuum-assisted oil/organic solvent adsorption system was designed to separate the mixture of toluene (100 mL) with 2 M HCl (100 mL), 2 M NaOH (100 mL), or saturated ( $\approx 26.5\%$  by weight) NaCl solution (100 mL).

## Supporting Information

Supporting Information is available from the Wiley Online Library or from the author.

## Acknowledgements

The authors appreciate the help of Dr. Michael Powell for XPS measurements. This work was financially supported by the National Basic Research Program of China (973 Program, grant NO. 2015CB057304), National Natural Science Foundation of China (Grant No. 51605078), Science Fund for Creative Research Groups of NSFC (51621064), and EPSRC project EP/G036675. F.C. thanks for the funding from China Scholarship Council (CSC) and the Fundamental Research Funds for the Central Universities. Y.L. and M.K.T. acknowledge the support from EPSRC project EP/N024915/1.

## Conflict of Interest

The authors declare no conflict of interest.

## Keywords

oil/water separation, PVDF, superhydrophobic, superoleophilic, table salt templates

Received: May 31, 2017

Revised: July 25, 2017

Published online:

- [1] a) D. Chen, H. Zhu, S. Yang, N. Li, Q. Xu, H. Li, J. He, J. Lu, *Adv. Mater.* **2016**, *28*, 10443; b) Q. Ma, Y. Yu, M. Sindoro, A. G. Fane, R. Wang, H. Zhang, *Adv. Mater.* **2017**, *29*, 1605361.
- [2] a) J. Ge, H. Y. Zhao, H. W. Zhu, J. Huang, L. A. Shi, S. H. Yu, *Adv. Mater.* **2016**, *28*, 10459; b) Q. Ma, H. Cheng, A. G. Fane, R. Wang, H. Zhang, *Small* **2016**, *12*, 2186; c) B. Wang, W. Liang, Z. Guo, W. Liu, *Chem. Soc. Rev.* **2015**, *44*, 336; d) Y. Yu, H. Chen, Y. Liu, V. S. Craig, Z. Lai, *Adv. Colloid Interface Sci.* **2016**, *235*, 46.
- [3] a) J. Ge, J. Zhang, F. Wang, Z. Li, J. Yu, B. Ding, *J. Mater. Chem. A* **2017**, *5*, 497; b) Q. Zhang, Y. Cao, N. Liu, W. Zhang, Y. Chen, X. Lin, Y. Wei, L. Feng, L. Jiang, *J. Mater. Chem. A* **2016**, *4*, 18128; c) A. K. Kota, G. Kwon, W. Choi, J. M. Mabry, A. Tuteja, *Nat. Commun.* **2012**, *3*, 1025; d) G. Kwon, A. K. Kota, Y. Li, A. Sohani, J. M. Mabry, A. Tuteja, *Adv. Mater.* **2012**, *24*, 3666.
- [4] a) X. Gui, J. Wei, K. Wang, A. Cao, H. Zhu, Y. Jia, Q. Shu, D. Wu, *Adv. Mater.* **2010**, *22*, 617; b) Q. Zhu, Q. Pan, F. Liu, *J. Phys. Chem. C* **2011**, *115*, 17464; c) X. Y. Zhang, Z. Li, K. S. Liu, L. Jiang, *Adv. Funct. Mater.* **2013**, *23*, 2881; d) B. Shang, Y. Wang, B. Peng, Z. Deng, *J. Colloid Interface Sci.* **2016**, *482*, 240; e) Z. Niu, J. Chen, H. H. Hng, J. Ma, X. Chen, *Adv. Mater.* **2012**, *24*, 4144; f) P. Calcagnile, D. Fragouli, I. S. Bayer, G. C. Anyfantis, L. Martiradonna, P. D. Cozzoli, R. Cingolani, A. Athanassiou, *ACS Nano* **2012**, *6*, 5413.
- [5] a) Z. Wang, P. Jin, M. Wang, G. Wu, C. Dong, A. Wu, *ACS Appl. Mater. Interfaces* **2016**, *8*, 32862; b) H. Bi, Z. Yin, X. Cao, X. Xie, C. Tan, X. Huang, B. Chen, F. Chen, Q. Yang, X. Bu, X. Lu, L. Sun, H. Zhang, *Adv. Mater.* **2013**, *25*, 5916; c) H. P. Cong, X. C. Ren, P. Wang, S. H. Yu, *ACS Nano* **2012**, *6*, 2693.
- [6] J. Ge, Y. D. Ye, H. B. Yao, X. Zhu, X. Wang, L. Wu, J. L. Wang, H. Ding, N. Yong, L. H. He, S. H. Yu, *Angew. Chem. Int. Ed.* **2014**, *53*, 3612.
- [7] a) H. Wang, E. Wang, Z. Liu, D. Gao, R. Yuan, L. Sun, Y. Zhu, *J. Mater. Chem. A* **2015**, *3*, 266; b) N. Cao, B. Yang, A. Barras, S. Szunerits, R. Boukherroub, *Chem. Eng. J.* **2017**, *307*, 319; c) F. Beshkar, H. Khojasteh, M. Salavati-Niasari, *J. Colloid Interface Sci.* **2017**, *497*, 57.
- [8] a) G.-D. Kang, Y.-M. Cao, *J. Membr. Sci.* **2014**, *463*, 145; b) F. Liu, N. A. Hashim, Y. Liu, M. R. M. Abed, K. Li, *J. Membr. Sci.* **2011**, *375*, 1.
- [9] W. Zhang, Z. Shi, F. Zhang, X. Liu, J. Jin, L. Jiang, *Adv. Mater.* **2013**, *25*, 2071.
- [10] Y. Yu, H. Chen, Y. Liu, V. S. J. Craig, C. Wang, L. H. Li, Y. Chen, *Adv. Mater. Interfaces* **2015**, *2*, 1400267.
- [11] A. K. An, J. Guo, E.-J. Lee, S. Jeong, Y. Zhao, Z. Wang, T. Leiknes, *J. Membr. Sci.* **2017**, *525*, 57.
- [12] a) D. A. Zha, S. L. Mei, Z. Y. Wang, H. J. Li, Z. J. Shi, Z. X. Jin, *Carbon* **2011**, *49*, 5166; b) T. Wu, Y. Pan, L. Li, *Colloids Surf., A* **2011**, *384*, 47; c) Y. Yu, H. Chen, Y. Liu, V. S. J. Craig, L. H. Li, Y. Chen, A. Tricoli, *Polymer* **2014**, *55*, 5616; d) B. N. Sahoo, K. Balasubramanian, *RSC Adv.* **2015**, *5*, 6743; e) R. Arora, K. Balasubramanian, *RSC Adv.* **2014**, *4*, 53761; f) M. Tao, L. Xue, F. Liu, L. Jiang, *Adv. Mater.* **2014**, *26*, 2943; g) W. Zhang, Y. Zhu, X. Liu, D. Wang, J. Li, L. Jiang, J. Jin, *Angew. Chem. Int. Ed.* **2014**, *53*, 856; h) M. Peng, H. Li, L. Wu, Q. Zheng, Y. Chen, W. Gu, *J. Appl. Polym. Sci.* **2005**, *98*, 1358.

- [13] a) F. Chen, J. L. Song, Z. Liu, J. Y. Liu, H. X. Zheng, S. Huang, J. Sun, W. J. Xu, X. Liu, *ACS Sustainable Chem. Eng.* **2016**, *4*, 6828; b) Y. Li, Z. Zhang, M. Wang, X. Men, Q. Xue, *J. Mater. Chem. A* **2017**, *5*, 5077; c) S. K. Zhou, P. P. Liu, M. Wang, H. Zhao, J. Yang, F. Xu, *ACS Sustainable Chem. Eng.* **2016**, *4*, 6409; d) A. A. Chavan, J. Pinto, I. Liakos, I. S. Bayer, S. Lauciello, A. Athanassiou, D. Fragouli, *ACS Sustainable Chem. Eng.* **2016**, *4*, 5495.
- [14] a) A. Tuteja, W. Choi, M. Ma, J. M. Mabry, S. A. Mazzella, G. C. Rutledge, G. H. McKinley, R. E. Cohen, *Science* **2007**, *318*, 1618; b) A. K. Kota, Y. Li, J. M. Mabry, A. Tuteja, *Adv. Mater.* **2012**, *24*, 5838; c) M. K. Tiwari, I. S. Bayer, G. M. Jursich, T. M. Schutzius, C. M. Megaridis, *ACS Appl. Mater. Interfaces* **2010**, *2*, 1114; d) S. Barroso-Solares, M. G. Zahedi, J. Pinto, G. Nanni, D. Fragouli, A. Athanassiou, *RSC Adv.* **2016**, *6*, 71100.
- [15] R. E. Sousa, J. C. C. Ferreira, C. M. Costa, A. V. Machado, M. M. Silva, S. Lancers-Mendez, *J. Polym. Sci., Part B: Polym. Phys.* **2015**, *53*, 761.
- [16] a) H. Y. Wang, Z. J. Liu, E. Q. Wang, R. X. Yuan, D. Gao, X. G. Zhang, Y. J. Zhu, *Appl. Surf. Sci.* **2015**, *332*, 518; b) Y. Zhu, W. Xie, F. Zhang, T. Xing, J. Jin, *ACS Appl. Mater. Interfaces* **2017**, *9*, 9603.
- [17] H. P. Srivastava, G. Arthanareeswaran, N. Anantharaman, V. M. Starov, *Desalination* **2011**, *283*, 169.
- [18] T. Sultana, G. L. Georgiev, G. Auner, G. Newaz, H. J. Herfurth, R. Patwa, *Appl. Surf. Sci.* **2008**, *255*, 2569.
- [19] a) C. M. Chang, Y. L. Liu, *Carbon* **2010**, *48*, 1289; b) T. I. T. Okpalugo, P. Papakonstantinou, H. Murphy, J. McLaughlin, N. M. D. Brown, *Carbon* **2005**, *43*, 153.
- [20] C. Yu, C. Yu, L. Cui, Z. Song, X. Zhao, Y. Ma, L. Jiang, *Adv. Mater. Interfaces* **2017**, *4*, 1600862.
- [21] a) Z. Y. Wu, C. Li, H. W. Liang, J. F. Chen, S. H. Yu, *Angew. Chem. Int. Ed.* **2013**, *52*, 2925; b) W. Lei, D. Portehault, D. Liu, S. Qin, Y. Chen, *Nat. Commun.* **2013**, *4*, 1777.
- [22] S. J. Choi, T. H. Kwon, H. Im, D. I. Moon, D. J. Baek, M. L. Seol, J. P. Duarte, Y. K. Choi, *ACS Appl. Mater. Interfaces* **2011**, *3*, 4552.
- [23] H. Bi, X. Xie, K. Yin, Y. Zhou, S. Wan, L. He, F. Xu, F. Banhart, L. Sun, R. S. Ruoff, *Adv. Funct. Mater.* **2012**, *22*, 4421.
- [24] a) L. P. Xu, X. Wu, J. Meng, J. Peng, Y. Wen, X. Zhang, S. Wang, *Chem. Commun.* **2013**, *49*, 8752; b) L. Xu, G. Xiao, C. Chen, R. Li, Y. Mai, G. Sun, D. Yan, *J. Mater. Chem. A* **2015**, *3*, 7498; c) A. Turco, C. Malitesta, G. Barillaro, A. Greco, A. Maffezzoli, E. Mazzotta, *J. Mater. Chem. A* **2015**, *3*, 17685.
- [25] a) M. Tao, L. Xue, F. Liu, L. Jiang, *Adv. Mater.* **2014**, *26*, 2943; b) J. Song, Y. Lu, J. Luo, S. Huang, L. Wang, W. Xu, I. P. Parkin, *Adv. Mater. Interfaces* **2015**, *2*, 1500350; c) Q. Zhu, Q. Pan, F. Liu, *J. Phys. Chem.* **2011**, *115*, 17464.
- [26] Y. Yang, H. Yi, C. Wang, *ACS Sustainable Chem. Eng.* **2015**, *3*, 3012.
- [27] J. Zhang, B. Li, L. Li, A. Wang, *J. Mater. Chem. A* **2016**, *4*, 2069.
- [28] a) A. Zhang, M. Chen, C. Du, H. Guo, H. Bai, L. Li, *ACS Appl. Mater. Interfaces* **2013**, *5*, 10201; b) X. Zhao, L. Li, B. Li, J. Zhang, A. Wang, *J. Mater. Chem. A* **2014**, *2*, 18281.
- [29] D. N. H. Tran, S. Kabiri, T. R. Sim, D. Losic, *Environ. Sci.: Water Res. Technol.* **2015**, *1*, 298.